

Tribological properties of vanadium oxides investigated with reactive molecular dynamics

Miljan Dašić^{a,b,*}, Ilia Ponomarev^{a,**}, Tomas Polcar^a, Paolo Nicolini^a

^a Department of Control Engineering, Faculty of Electrical Engineering, Czech Technical University in Prague, Technická 2, Prague 6, 16627, Czech Republic

^b Scientific Computing Laboratory, Center for the Study of Complex Systems, Institute of Physics Belgrade, University of Belgrade, Pregrevica 118, Belgrade, 11080, Serbia

ARTICLE INFO

Keywords:

Lubrication
Hard coatings
Vanadium oxides
Molecular dynamics
ReaxFF

ABSTRACT

We present a reactive molecular dynamics study on tribological properties of five vanadium oxides (V_2O_3 , V_3O_5 , V_8O_{15} , V_9O_{17} , VO_2) under elevated temperatures and pressures. All considered stoichiometries provide lubrication with a comparatively low coefficient of friction ($COF \sim 0.2$ at 600 K, $COF < 0.2$ at 800 and 1000 K) which is a valuable information relevant for the design of coatings containing vanadium as a lubricious agent. An overall tendency of the decrease of friction coefficient with the increase of temperature represents a tribological effect useful for self-adjusting lubrication. We observed the increasing trend of adhesion-related offset of the friction force with the decrease of oxygen content in vanadium oxides.

1. Introduction

Friction and wear represent a serious obstacle to the efficient operation of engineering systems in all areas of industry. There is an estimate that friction and wear cause a loss of approximately one-quarter of the global energy production [1]. In every system where a contact between surfaces in relative motion is present, the phenomenon of friction occurs and causes energy losses. Considering this fact, the usage of materials, referred to as *lubricants*, which can enable low friction and prevent wear, is necessary [2].

The most common choices include *liquid lubricants* like water-based ones [3–6], petroleum-based oils [7–9], or ionic liquids [10–14]. When it comes to more specific operating conditions, including high temperature or vacuum, *solid lubricants* need to be used instead of liquid ones. The two major families include *carbon-based* solid lubricants (such as graphite [15–17] or diamond-like carbon coatings [18,19]) and *transition metal dichalcogenides* (TMDs) [20–24]. However, both of them show a tendency to degrade at elevated temperatures in oxidative environment [25,26].

Taking into account that providing effective lubrication at high temperatures/pressures and under oxidation is relevant for various industrial applications, such as turbomachinery and cutting tools [27, 28], there is a need for designing suitable coatings. Those are hard and oxidation-resistant coatings consisting of binary or ternary films (e.g., Cr–N, Ti–N, Cr–Al–N, Ti–Al–N), doped with an additional element

(usually a metal) [27–33]. Such coatings operate in a way that the dopant diffuses to the surface of the coating, reacts with oxygen, and forms an oxide layer that serves as a lubricant. Out of several possibilities for the choice of the metal, *vanadium* and *silver* gained popularity. There is either oxide (V–O) or metallic (Ag) lubrication. Vanadium oxides and metallic silver reduce friction and melt at relatively low temperatures (below 700 °C in case of V_2O_5 ; melting point of metallic Ag is 961.8 °C, both at atmospheric pressure), hence providing liquid lubrication [28,32,34–39].

We have previously studied the tribological properties of vanadium pentoxide V_2O_5 [40]. We found out that even a single layer of it present on the surface of a vanadium doped solid lubricant provides efficient lubrication with the coefficient of friction $COF < 0.2$, which is an established value when considering lubrication based on solid-lubricating materials [26].

The dopant of solid coatings investigated in the present study is *vanadium* (as in the Ref. [40]), which reacts with oxygen and forms oxides with different stoichiometries, depending on the working conditions [41]. Accordingly, the amount of oxygen present in the oxidative environment, can be taken as a study parameter, leading to the consideration of different vanadium-oxide stoichiometries.

This study aims to explore the tribological performance of under-oxidized vanadium lubricants. The key questions which we are targeting are related to the usability (i.e., providing lubrication regardless

* Corresponding author at: Scientific Computing Laboratory, Center for the Study of Complex Systems, Institute of Physics Belgrade, University of Belgrade, Pregrevica 118, Belgrade, 11080, Serbia.

** Corresponding author.

E-mail addresses: dasicmil@fel.cvut.cz, mdasic@ipb.ac.rs (M. Dašić), ponomili@fel.cvut.cz (I. Ponomarev).

<https://doi.org/10.1016/j.triboint.2022.107795>

Received 7 April 2022; Received in revised form 11 July 2022; Accepted 17 July 2022

Available online 25 July 2022

0301-679X/© 2022 Elsevier Ltd. All rights reserved.

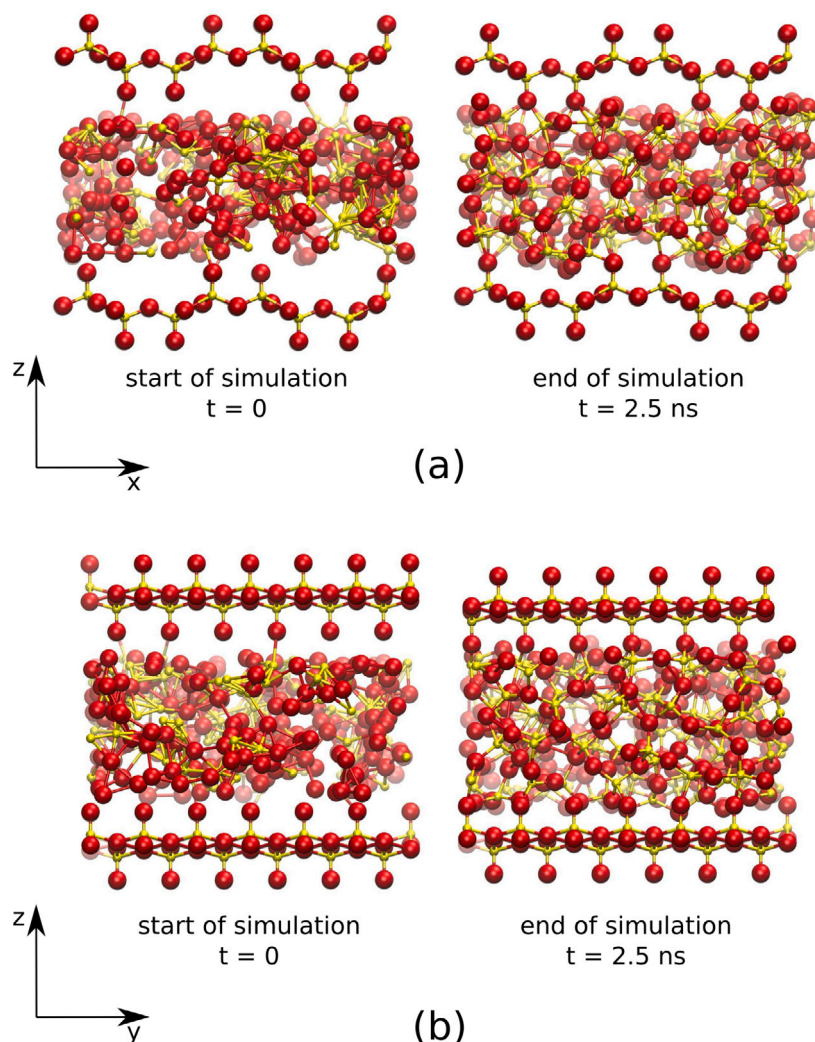


Fig. 1. Snapshots ((a) xz and (b) yz cross-sections) of the simulated tribological system taken at the start ($t = 0$) and at the end ($t = 2.5$ ns) of a simulation. Vanadium and oxygen atoms are represented as smaller yellow and bigger red spheres, respectively. The top and bottom V_2O_5 layer represent rigid counter-bodies, while V and O atoms confined between them constitute a vanadium oxide lubricant of a certain stoichiometry, in general labelled as V_xO_y .

of the stoichiometry) and efficiency (i.e., enabling low friction coefficient) of such lubricants. We have conducted a reactive molecular dynamics study on the tribological properties of five vanadium oxide stoichiometries. Our study includes V_2O_3 , V_3O_5 , V_8O_{15} , V_9O_{17} , VO_2 , which are observed in experimental investigations of coatings with vanadium oxide-based lubrication [37,41,42].

2. Methods

We have employed an atomistic model within the *ReaxFF* (reactive force field) potential [43] to describe the interactions of vanadium and oxygen atoms. *ReaxFF* is an empirical potential based on the bond order concept. The total potential energy of the system is calculated as a sum of energies of different components: bonds, atoms, lone-pairs, valence and torsion angles, hydrogen bonds, van der Waals and Coulombic interactions. *ReaxFF* uses bond orders which change dynamically during the simulation, depending on the interatomic distances.

In this study, we used the *Chenoweth et al.* force field parameterization [44], which was originally developed for oxidative dehydrogenation on vanadium oxide catalysts. Besides that purpose, the aforementioned force field has been used to study the chemical stability and surface stoichiometry of solid vanadium oxide phases [45]. Also, the *Chenoweth et al.* force field has been used in a study on the tribological properties of crystalline and amorphous V_2O_5 lubricants [40].

All reactive molecular dynamics simulations presented in this work have been conducted using the *reax/c* package [46] of the *LAMMPS* code [47,48].

Since the main target of our study is the exploration of the effects of stoichiometry on the tribological properties of vanadium oxides, our present simulation setup is designed analogously to the one utilized in a previous study on the mechanism of tribological action of V_2O_5 [40]. Such approach allows comparisons of the tribological performance of under-oxidized vanadium and vanadium pentoxide lubricants. Our tribological system consists of two V_2O_5 layers, which are used as rigid counter-bodies, and an initially random arrangement of $N_V = 144$ vanadium atoms and an appropriate number of oxygen atoms N_O , which are used as a lubricant confined between the two V_2O_5 layers. The above-mentioned term *appropriate* means that the number of oxygen atoms is determined in correspondence with the chosen stoichiometry of vanadium oxides, which is in general labelled as V_xO_y , hence $N_O = \frac{y}{x}N_V$. The mass density of considered V_xO_y phases was selected in a way that it is equal to the mass density of the corresponding crystalline vanadium oxide, minus 10% to account for a lower density of the amorphous phase. Regarding the periodic boundary conditions applied, our system was periodic in all three directions (i.e., x , y and z), however in the z direction we effectively had rigid layers acting like walls.

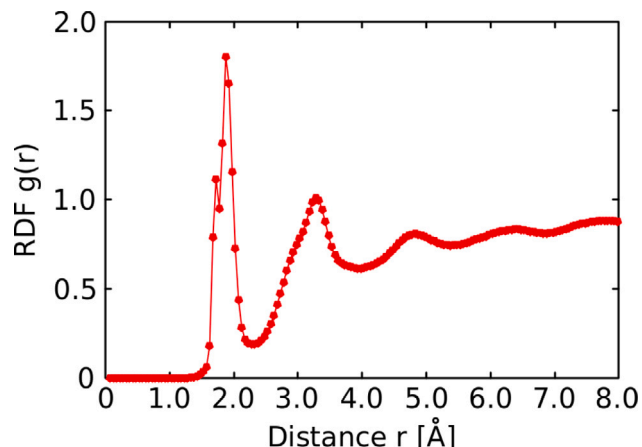


Fig. 2. Representative total radial distribution function (RDF), labelled as $g(r)$, for the set of parameters (V_3O_5 , 4 GPa, 1000 K). For all sets of parameters the RDFs have a similar dependence on the distance, taking into account the presence of short-range and the lack of long-range ordering (check Figs. 3, 4 in Supplementary Information).

The first step of our simulations was a *structural relaxation* of the initially randomly arranged V_xO_y phase, where we applied the conjugate gradient method within LAMMPS [47,48], with the stopping tolerance of 10^{-12} for energy and 10^{-12} kcal/molÅ for force; both maximum number of iterations of minimizer and maximum number of force/energy evaluations were set at 10^5 . After the relaxation, we proceeded to a *melt-quench* step at a target normal load of 0, 1, 2, 3 or 4 GPa, imposed on the top rigid V_2O_5 layer. We heated the V_xO_y phase up to 5000 K and then quenched it at a rate of -10 K/ps to the target temperature of 600 K, 800 K or 1000 K. After these steps, we proceeded with the system *equilibration* at the target temperature for 100 ps, and then we started the *sliding* of the top V_2O_5 layer in the x -direction at a velocity of $V_x = 1.133$ m/s. We chose the sliding velocity so that 1 ns of sliding corresponds to a run through the primitive cell of V_2O_5 , which is consistent with our previous study [40]. The sliding part of our simulations lasted for 2 ns and during this production stage we recorded the atomic positions and forces, so that they can be used in a subsequent analysis. In all simulations, we used a timestep of 0.5 fs. For any simulation conditions (comprising selected stoichiometry, applied normal load and temperature), 5 independent runs were carried out. Different independent runs correspond to the usage of different seeds of the random number generator applied to obtain the starting configurations of the confined V and O atoms in the V_xO_y phase. Such

a procedure enabled us to determine the averages and the standard deviations of the computed quantities. An illustration of our simulation setup at the start and at the end of a simulation is shown in Fig. 1.

3. Results and discussion

3.1. Tribological behaviour of amorphous vanadium oxides

Let us label the set of parameters defining a distinguishable simulation as (V_xO_y, F_z, T, i) , which correspond to the stoichiometry, normal load, temperature and index of the independent run, respectively. The friction force was defined as the force acting on the top rigid V_2O_5 layer in the direction opposite to the sliding direction; hence, we label it as F_x . For each set of parameters (V_xO_y, F_z, T) we determine the friction force by computing the average value over five independent runs. The associated error was computed as the unbiased standard deviation over the independent runs.

In Fig. 2 we show the total radial distribution function related to the sliding segment of our simulations for the representative set of parameters (V_3O_5 , 4 GPa, 1000 K). The results are analogous for all sets of parameters. We notice a short-range ordering, arising from distinct (though not fixed) bonding distances, but any long-range ordering is lacking, identifying our V_xO_y phase as *amorphous* or *liquid*. The boundary between an *amorphous solid* and a *liquid* state is not clearly and straightforwardly distinguishable, especially considering the working conditions of our study (i.e., relatively high temperatures and normal loads, together with sliding). Taking all relevant circumstances into account, we consider those two states as equivalent within the framework of our study.

In Fig. 3 we present the evolution of the sliding force with respect to time for the set of parameters (V_3O_5 , 4 GPa, 1000 K). It is a representative case for the sliding force vs. time relationship; the profiles for other sets of parameters look qualitatively similar to the reported one. We can notice in Fig. 3(a) the absence of upward/downward trends, which implies that the system undergoes a steady sliding process. This kind of tribological behaviour is expected for amorphous/liquid lubricants, differently from, for example, crystalline V_2O_5 lubricant [40]. In Fig. 3(b) we show the temporal trends (computed as the moving average over 1000 values) of all five independent runs. Qualitatively, in all 5 cases the sliding force vs. time curves are analogous.

By following the standard approach in tribology, we applied a linear fitting on the dependence of the sliding force F_x on the normal load F_z :

$$F_x = COF \cdot F_z + F_x^0, \quad (1)$$

where the slope corresponds to the coefficient of friction (COF), while the offset F_x^0 corresponds to the sliding force when the normal load on

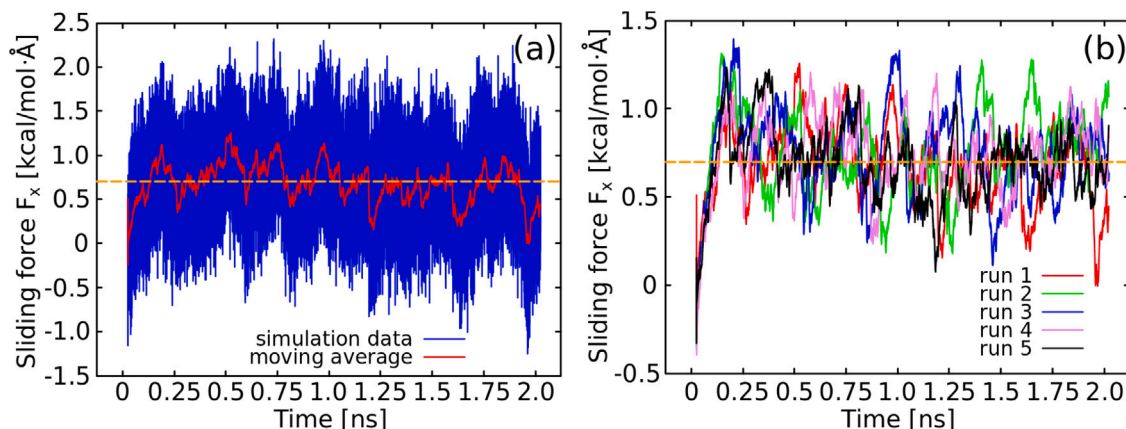


Fig. 3. Time profiles of the sliding force F_x in the case of V_3O_5 lubricant under the applied pressure of 4 GPa and at the temperature of 1000 K. Panel (a) reports the results of the independent run 1. In the panel (a), the solid blue line represents raw simulation data, the solid red line represents the moving average, while the horizontal dashed orange line is the global average. Panel (b) shows the moving averages of the sliding force corresponding to the 5 independent runs, represented by solid lines with different colours. It also includes the global average calculated over all 5 independent runs (for the same set of parameters (V_3O_5 , 4 GPa, 1000 K)), marked with a horizontal dashed orange line.

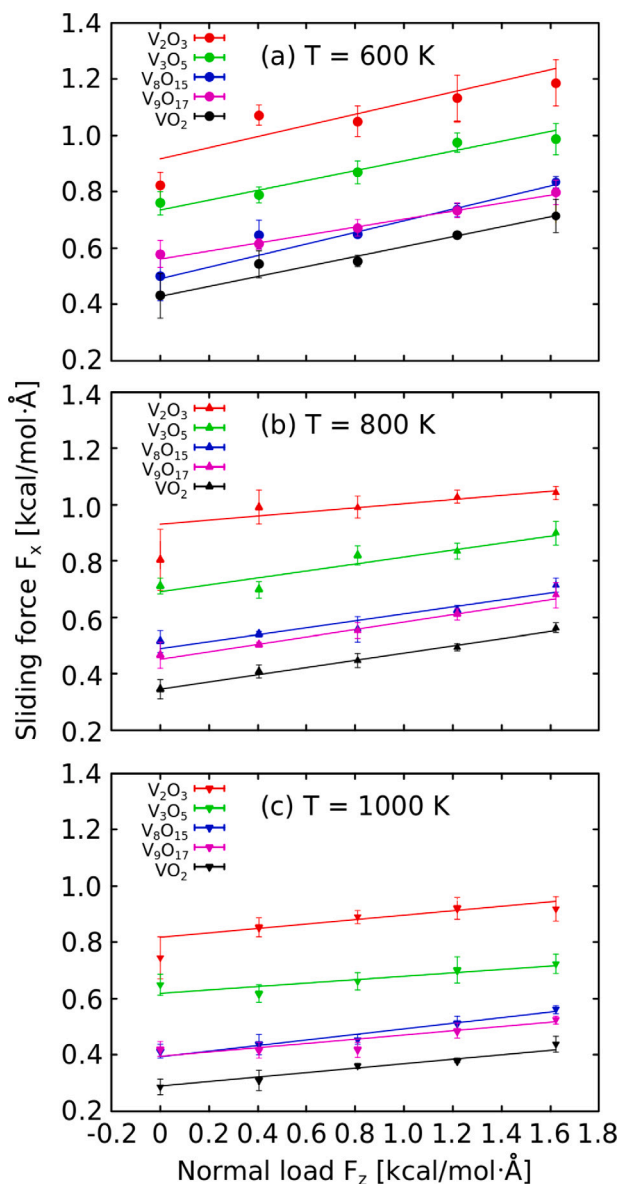


Fig. 4. Dependence of the sliding force F_x on the normal load F_z at the temperatures of (a) $T = 600$ K, (b) $T = 800$ K and (c) $T = 1000$ K. The error bars represent the standard deviation of the average values obtained from the sliding simulations. The solid lines were obtained by linear fitting via Eq. (1). Corresponding parameters of the applied linear fitting are listed in Table I of the Supplementary Information.

the top V_2O_5 layer is not applied (i.e., $F_z = 0$). In Fig. 4 we present the sliding force F_x vs. normal load F_z dependence for all considered stoichiometries and temperatures. We can notice the effects of stoichiometry and temperature on the frictional behaviour of amorphous vanadium oxide lubricants: there is a separation and ordering of the results (i.e., the offset of the linear fits) depending on the stoichiometry; temperature affects both the slope and the offset of the linear fits.

To gain a more detailed insight into the dependence of the slope and offset of applied linear fits (from Eq. (1)) on the stoichiometry and temperature, we prepared the COF and F_x^0 vs. stoichiometry plots at all studied temperatures, shown in Fig. 5(a) and Fig. 5(b), respectively. At a fixed temperature, we do not notice any statistically significant changes of the COF as a function of stoichiometry. The values which we obtained for the COF (~ 0.2 at 600 K, ~ 0.15 at 800 K and ~ 0.1 at 1000 K) are also in good agreement with the previously determined results for amorphous V_2O_5 lubricant at the same temperatures

(e.g., see Fig. 8 and Table 6 in the Ref. [40]), which means that even under-oxidized vanadium is going to be an effective lubricant. There is also an overall tendency of the decrease of COF with the increase of temperature for all considered vanadium oxides, however, in some cases the values of COF at different temperatures are indistinguishable within the margin of error. The decrease of friction coefficient with the increase of temperature is an expected tribological effect in the case of the hydrodynamic lubrication regime of the Stribeck curve [49]. A higher temperature of an amorphous/liquid lubricant leads to its lower viscosity [50,51] and, consequently, to a lower friction coefficient. Another consequence of such behaviour is a somewhat self-adjusting character of the lubrication, which enables lowering of the friction coefficient. Sliding at a lower temperature with a higher COF would generate energy, dissipated in the form of heat, that would, in turn, increase the temperature of the coating and hence decrease the COF , allowing easier sliding. We added a dashed horizontal line in Fig. 5(a) at $COF = 0.2$ to denote an established boundary for the low value of the friction coefficient of high-temperature self-lubricating coatings. Such a boundary low value can be used for defining the quality of novel solid-lubricating materials (e.g., see Fig. 5 in the Ref. [26]). All the obtained values of COF at the temperatures of 800 and 1000 K are well-below this threshold of 0.2, while at 600 K the values belong to its vicinity. We should mention that there is a good agreement of our results regarding COF with the values of experimentally measured COF of vanadium-containing nitride coatings [29,37,52].

The offset F_x^0 of the linear fits from Eq. (1) is related to the adhesion component of the friction force [53–55]. In Fig. 5(b) we present the F_x^0 vs. stoichiometry dependence for the three studied temperatures. We notice an overall decreasing trend of the F_x^0 with the increase of the oxidation level of vanadium. As F_x^0 accounts for the adhesion between the top rigid V_2O_5 layer and the V_xO_y lubricant, a higher oxidation level of vanadium in V_xO_y , enables formation of less bonds between the V_2O_5 layer and the lubricant, which leads to a lower adhesion. This represents mainly a qualitative explanation of the adhesion-stoichiometry relation. However, we provide a quantitative explanation based on counting the bonds between the V_xO_y lubricant and the top V_2O_5 layer in the following subsection titled *Structural analysis*.

As already stated in the *Methods* section, our simulation setup was built with the V_2O_5 layers as counter-bodies of the tribo-contact to make the results comparable with the previous study [40] dealing with the amorphous V_2O_5 lubricant. However, such a simulation setup can also be somewhat relevant for practical applications. In the operation of a real coating, utilized for example, as a cutting tool, we would expect the tribolayer of vanadium oxides to be sandwiched between the products of oxidation of the coating (primarily oxides like SiO_2 and TiO_2) and the surface of the stainless steel, which is also an oxidized surface. Even though our molecular dynamics model is far from perfect to simulate such interactions, it might show some relevant trends. In the applications like coatings for cutting tools, adhesion can be a very important phenomenon since the cutting tool should not be stuck on the surface.

3.2. Structural analysis

We have defined a V–O bond as V and O atoms being closer than the cutoff distance of 2.5 Å, which is the length of the longest V–O bond in crystalline oxides (2.2 Å, in ReaxFF-optimized V_2O_5), plus extra 15% to account for generally longer bonds in amorphous phase [56]. We looked at a number of V–O bonds, expressed as the average coordination numbers of vanadium, CN_V , and oxygen, CN_O . We paid special attention to the bonding between the rigid V_2O_5 layers and the amorphous V_xO_y oxide phase. These bonds are almost exclusively formed between the V atoms of the amorphous V_xO_y phase and the O atoms of the rigid V_2O_5 layers. Consideration of the aforementioned bonds provides us a good measure of the adhesion interactions between a rigid oxide body and an amorphous oxide. We quantify this type of

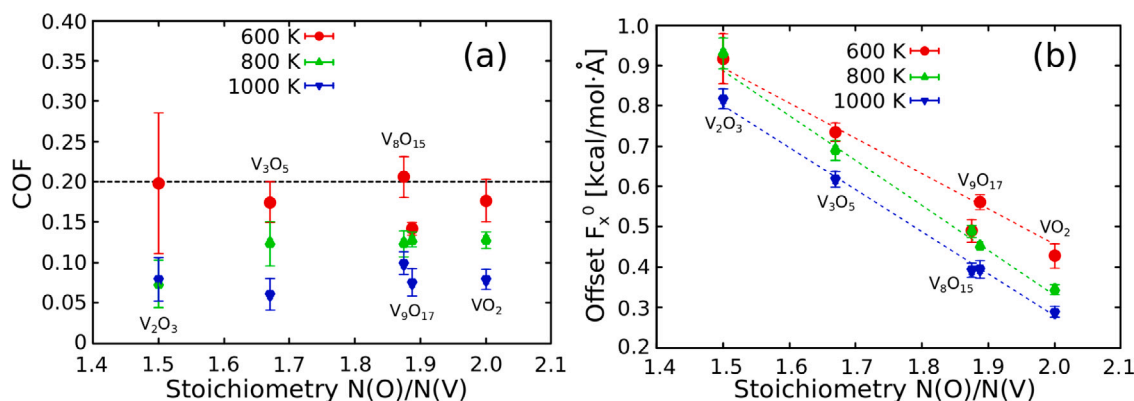


Fig. 5. (a) Dependence of the friction coefficient COF on the stoichiometry at the temperatures of $T = \{600, 800, 1000\}$ K. (b) Dependence of the offset of the sliding force F_x^0 on the stoichiometry at the temperatures of $T = \{600, 800, 1000\}$ K. The points presented in the panels (a) and (b) were obtained as slopes and offsets of the linear fits from Eq. (1), respectively, while the errorbars represent the associated error computed via the fitting procedure. Dashed lines in the panel (b) represent linear fits, that serve as guides to the eye.

bonding as the number of such bonds per a V atom, and denote it as CN_V^* .

We have seen from Fig. 5(a) that the stoichiometry of amorphous vanadium oxide lubricants weakly affects the friction coefficient. However, it clearly impacts the offset of the sliding force F_x^0 , as we can observe from Fig. 5(b). This effect can also be noticed in the separation and ordering, with respect to stoichiometry, of the sliding force vs. normal load curves in Fig. 4. In order to quantitatively describe such a behaviour, we analysed the structural features of V_xO_y phases, looking primarily into V–O bonds.

The effect of stoichiometry on the network connectivity and the occurrence of such V_xO_y -to- V_2O_5 bonds at the temperature of 1000 K (results for the other two studied temperatures are analogous) is presented in Fig. 6. We observe the almost constant coordination numbers of vanadium ($CN_V \sim 4$ under the normal load of 0 GPa) throughout the stoichiometries. On the other side, the coordination number of oxygen CN_O decreases with the increase of the overall oxygen content in the V_xO_y phase, in order to provide enough bonding to vanadium. Also, as we move to more oxygen-poor stoichiometries, we observe a higher tendency of the vanadium atoms from V_xO_y to bond with the oxygen atoms from V_2O_5 rigid layers, i.e., CN_V^* increases. Since those bonds are to be considered the main cause of the adhesion between the V_xO_y lubricant and the rigid V_2O_5 layers, this tendency offers an explanation for the increase of the offset of the sliding force F_x^0 with the decrease of the oxygen content in V_xO_y , as shown in Fig. 5(b). Also, we obtained that, at a fixed stoichiometry, all coordination numbers (i.e., CN_V , CN_V^* and CN_O) increase with the increase of the normal load. This outcome can be easily explained taking into account that the increased normal load causes a closer contact of atoms in the V_xO_y lubricant (i.e., a lower volume per atom; see Fig. 1 in the Supplementary Information). Consequently, there are more atoms positioned within the bonding cutoff distance of 2.5 Å. As the oxygen content decreases, the overall increase of the average coordination number of oxygen causes the increase of the average V–O bond lengths, as we show it in Fig. 7. The elongation of the bonding distances lowers the bond energy, which makes bond switching in the course of sliding, and hence the changes in the network connectivity of the V_xO_y lubricant, easier. This might be a reason for the almost constant COF throughout the stoichiometries: there are more bonds per atom as the amount of oxygen in V_xO_y decreases (both by just increasing the fraction of atoms with a higher CN and by increasing the CN of oxygen atoms). However, those bonds are longer and, consequently, weaker. Hence, the opposite changes of the number of bonds and their length with respect to stoichiometry are the effects cancelling each other, which results in a weak dependence of the friction coefficient on stoichiometry (see Fig. 5(a)).

Similarly to a previous study (see Fig. 9 in Ref. [40]), we present the effect of the network connectivity of amorphous V_xO_y lubricant

(expressed as the average coordination number of vanadium CN_V) on the sliding force F_x in Fig. 8. As in the case of V_2O_5 , we observe a linear relation between the quantities in question, which is reasonable as a behaviour consistent with the fluid lubrication regime of the Stribeck curve [49]: higher network connectivity means higher viscosity [57, 58], which results in a higher friction force.

4. Conclusions

We have performed reactive molecular dynamics simulations to study the tribological properties of practically relevant vanadium oxide phases at elevated temperatures and pressures. Stoichiometries of vanadium oxides were selected in accordance with available experimental studies. Sliding simulations explored the tribocontact of two rigid V_2O_5 layers used as counter-bodies and a thermalized V_xO_y lubricant confined between them. Under the imposed working conditions, all vanadium oxides were amorphous.

In general, the available amount of oxygen in an oxidative environment in which a vanadium doped hard coating is used, might be insufficient to form V_2O_5 . The main goal of our study was to explore the effectiveness of vanadium-based lubricants at lower oxidation states; in other words: can they provide low friction in oxygen-poor environment. We found no noticeable differences in friction coefficients between various amorphous vanadium oxide phases. All of the studied vanadium oxides provide lubrication with a considerably low friction coefficient ($COF \sim 0.2$ at the temperature of 600 K, $COF < 0.2$ at the temperatures of 800 and 1000 K). We figured out that the friction coefficient decreases with the increase of the temperature, which can be favourable for self-adjusting lubrication in the tribological conditions, when the energy dissipation leads to the temperature increase.

We observed the increasing trend of the adhesion-related offset of the friction force with the decrease of the oxygen content and explained it by the more-pronounced tendency of vanadium atoms to bond with the oxygen atoms of the counter-bodies in oxygen-poorer environment. For all vanadium oxides we observed a linear relation between the friction force and the network connectivity, consistent with previous findings regarding V_2O_5 . We obtained an overall tendency of the increase in bond length and network connectivity with the increase of normal load, for all stoichiometries and at all studied temperatures.

As a concluding remark, our study on vanadium oxide lubricants provides a reliable reference relevant for the development of oxidation-resistant hard coatings containing vanadium as a lubricious element.

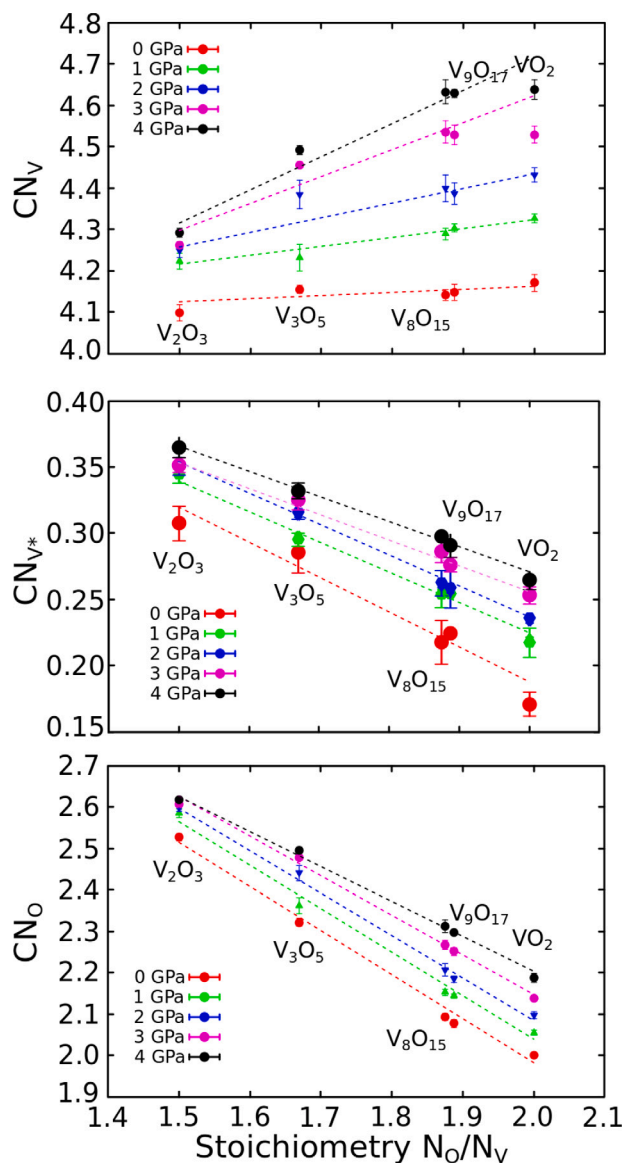


Fig. 6. Dependence of the average coordination numbers of vanadium (CN_V in the top and CN_{V^*} in the middle panel) and oxygen (CN_O in the bottom panel) on the stoichiometry at the temperature of 1000 K and under all applied normal loads. The results at 600 and 800 K are quantitatively similar (i.e., impact of the temperature within the studied range is negligible). The error bars represent the standard deviation of the average values obtained from the sliding simulations. Dashed lines were obtained by linear fitting and they serve as guides to the eye.

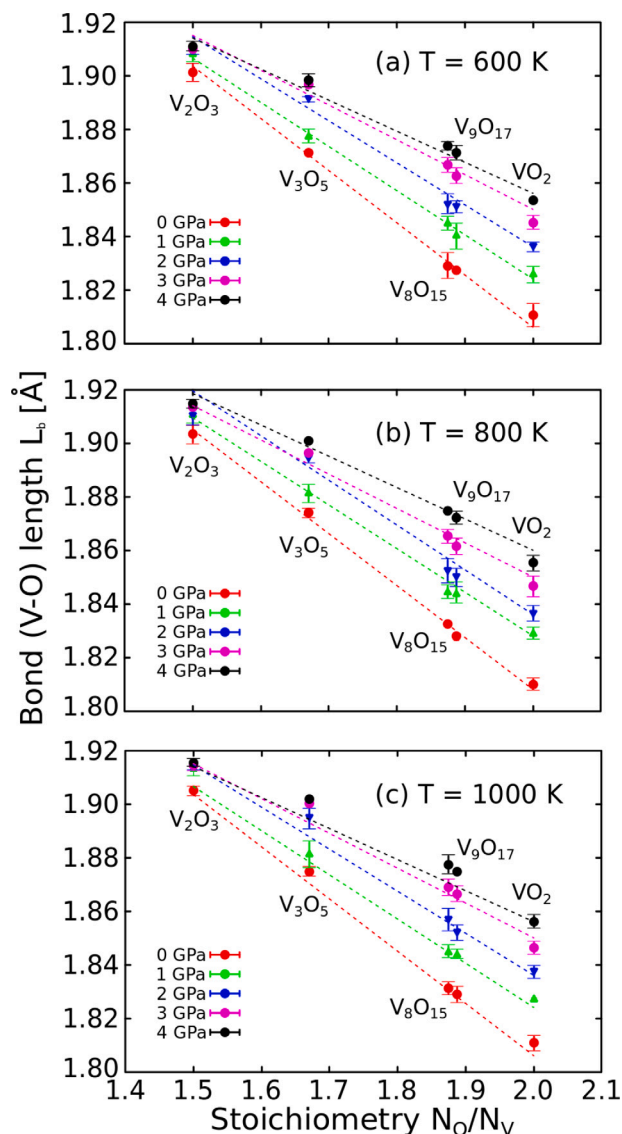


Fig. 7. Dependence of the average bond (V-O) length on the stoichiometry at the temperatures of (a) $T = 600$ K, (b) $T = 800$ K and (c) $T = 1000$ K and under all applied normal loads. The error bars represent the standard deviation of the average values obtained from the sliding simulations. Dashed lines were obtained by linear fitting and they serve as guides to the eye.

CRedit authorship contribution statement

Miljan Dašić: Methodology, Validation, Formal analysis, Investigation, Data curation, Writing – original draft, Writing – review & editing, Visualization. **Ilija Ponomarev:** Conceptualization, Methodology, Validation, Formal analysis, Investigation, Data curation, Writing – original draft, Writing – review & editing. **Tomas Polcar:** Resources, Writing – review & editing, Supervision, Funding acquisition. **Paolo Nicolini:** Conceptualization, Methodology, Resources, Writing – review & editing, Supervision, Project administration, Funding acquisition.

Declaration of competing interest

The authors declare that they have no known competing financial interests or personal relationships that could have appeared to influence the work reported in this paper.

Acknowledgements

The authors highly acknowledge the financial support of the Austrian Science Fund (FWF) under the project I 4059-N36 and the Czech Science Foundation under the project 19–29679 L. I.P. thanks the ESI Fund, Czech Republic and the OPR DE International Mobility of Researchers MSCA-IF III, Czech Republic at CTU in Prague (no. CZ.02.2.69/0.0/0.0/20_079/0017983) for their support. This work was supported by the Ministry of Education, Youth and Sports of the Czech Republic through the e-INFRA CZ (ID:90140). We acknowledge that the results of this research have been achieved using the DECI resource Kay based in Ireland at the Irish Centre for High-End Computing (ICHEC) with support from the PRACE AISBL. The use of VMD [59] software for the visualization of our tribological system (available at <http://www.ks.uiuc.edu/Research/vmd/>) is also acknowledged.

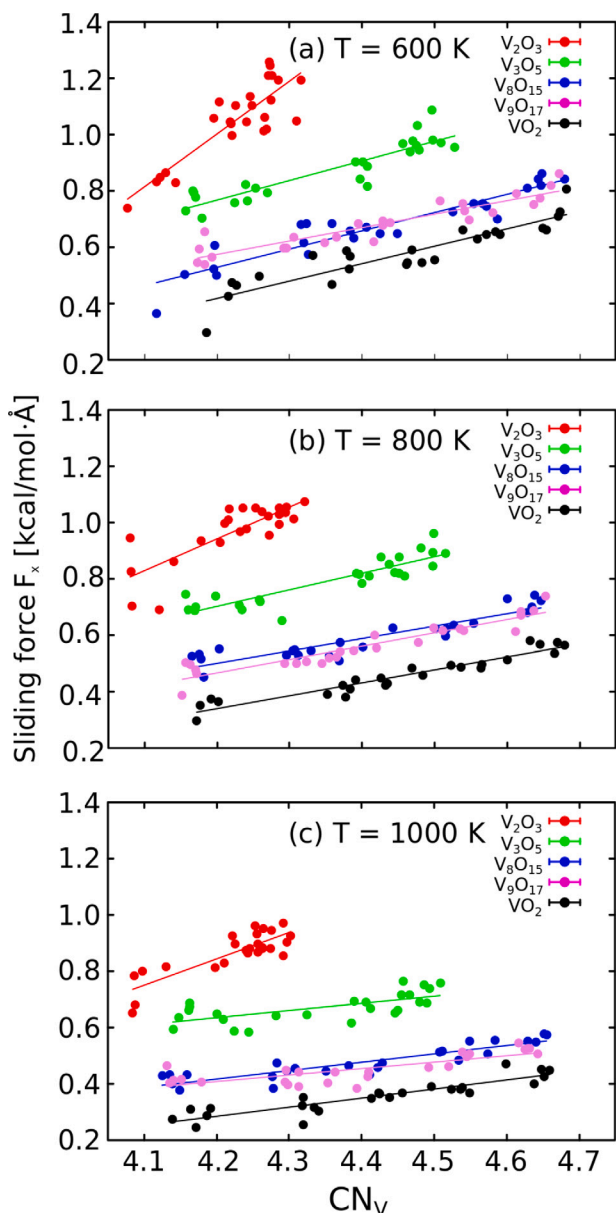


Fig. 8. Relation between the sliding force F_x and the average coordination number of vanadium CN_V at the temperatures of (a) $T = 600$ K, (b) $T = 800$ K and (c) $T = 1000$ K and for all considered vanadium oxide stoichiometries. Solid lines were obtained by linear fitting and they serve as guides to the eye, pointing out to a linear relation between F_x and CN_V .

Appendix A. Supplementary information

Supplementary material related to this article can be found online at <https://doi.org/10.1016/j.triboint.2022.107795>.

References

- [1] Holmberg K, Erdemir A. Influence of tribology on global energy consumption, costs and emissions. *Friction* 2017;5(3):263–84.
- [2] Mang T, Dresel W. *Lubricants and lubrication*. John Wiley & Sons; 2007.
- [3] Tomala A, Karpinska A, Werner W, Olver A, Störi H. Tribological properties of additives for water-based lubricants. *Wear* 2010;269(11–12):804–10.
- [4] Sagraloff N, Dobler A, Tobie T, Stahl K, Ostrowski J. Development of an oil free water-based lubricant for gear applications. *Lubricants* 2019;7(4):33.
- [5] Chen W, Amann T, Kailer A, Rühle J. Macroscopic friction studies of Alkylglucopyranosides as additives for water-based lubricants. *Lubricants* 2020;8(1):11.

- [6] Rahman MH, Warneke H, Webbert H, Rodriguez J, Austin E, Tokunaga K, et al. Water-based lubricants: Development, properties, and performances. *Lubricants* 2021;9(8):73.
- [7] Girotti G, Raimondi A, Blengini GA, Fino D. The contribution of lube additives to the life cycle impacts of fully formulated petroleum-based lubricants. *Am J Appl Sci* 2011;8(11):1232.
- [8] Raimondi A, Girotti G, Blengini GA, Fino D. Lca of petroleum-based lubricants: state of art and inclusion of additives. *Int J Life Cycle Assess* 2012;17(8):987–96.
- [9] Madanhire I, Mbohwa C. *Mitigating environmental impact of petroleum lubricants*. Springer; 2016.
- [10] Xiao H. Ionic liquid lubricants: basics and applications. *Tribol Trans* 2017;60(1):20–30.
- [11] Gkagkas K, Ponnuchamy V, Dašić M, Stanković I. Molecular dynamics investigation of a model ionic liquid lubricant for automotive applications. *Tribol Int* 2017;113:83–91.
- [12] Dašić M, Stanković I, Gkagkas K. Influence of confinement on flow and lubrication properties of a salt model ionic liquid investigated with molecular dynamics. *Eur Phys J E* 2018;41(11):1–12.
- [13] Dašić M, Stanković I, Gkagkas K. Molecular dynamics investigation of the influence of the shape of the cation on the structure and lubrication properties of ionic liquids. *Phys Chem Chem Phys* 2019;21(8):4375–86.
- [14] Cai M, Yu Q, Liu W, Zhou F. *Ionic liquid lubricants: When chemistry meets tribology*. Chem Soc Rev 2020.
- [15] Field S, Jarratt M, Teer D. Tribological properties of graphite-like and diamond-like carbon coatings. *Tribol Int* 2004;37(11–12):949–56.
- [16] Chen B, Bi Q, Yang J, Xia Y, Hao J. Tribological properties of solid lubricants (graphite, h-BN) for Cu-based P/M friction composites. *Tribol Int* 2008;41(12):1145–52.
- [17] Egea AS, Martynenko V, Abate G, Deferrari N, Krahmer DM, de Lacalle LL. Friction capabilities of graphite-based lubricants at room and over 1400 K temperatures. *Int J Adv Manuf Technol* 2019;102(5):1623–33.
- [18] Hauert R. An overview on the tribological behavior of diamond-like carbon in technical and medical applications. *Tribol Int* 2004;37(11–12):991–1003.
- [19] Erdemir A. Genesis of superlow friction and wear in diamondlike carbon films. *Tribol Int* 2004;37(11–12):1005–12.
- [20] Polcar T, Cavaleiro A. Review on self-lubricant transition metal dichalcogenide nanocomposite coatings alloyed with carbon. *Surf Coat Technol* 2011;206(4):686–95.
- [21] Yang J-F, Parakash B, Hardell J, Fang Q-F. Tribological properties of transition metal di-chalcogenide based lubricant coatings. *Front Mater Sci* 2012;6(2):116–27.
- [22] Nicolini P, Capozza R, Restuccia P, Polcar T. Structural ordering of molybdenum disulfide studied via reactive molecular dynamics simulations. *ACS Appl Mater Interfaces* 2018;10(10):8937–46.
- [23] Serpini E, Rota A, Valeri S, Ukrainsev E, Rezek B, Polcar T, Nicolini P. Nanoscale frictional properties of ordered and disordered MoS₂. *Tribol Int* 2019;136:67–74.
- [24] Rapuc A, Simonovic K, Huminiuc T, Cavaleiro A, Polcar T. Nanotribological investigation of sliding properties of transition metal dichalcogenide thin film coatings. *ACS Appl Mater Interfaces* 2020;12(48):54191–202.
- [25] Zhang S, Bui XL, Li X. Thermal stability and oxidation properties of magnetron sputtered diamond-like carbon and its nanocomposite coatings. *Diam Relat Mater* 2006;15(4–8):972–6.
- [26] Zhu S, Cheng J, Qiao Z, Yang J. High temperature solid-lubricating materials: A review. *Tribol Int* 2019;133:206–23.
- [27] Papi PA, Mulligan C, Gall D. Cr-N-Ag nanocomposite coatings: control of lubricant transport by diffusion barriers. *Thin Solid Films* 2012;524:211–7.
- [28] Voevodin AA, Muratore C, Aouadi SM. Hard coatings with high temperature adaptive lubrication and contact thermal management. *Surf Coat Technol* 2014;257:247–65.
- [29] Fateh N, Fontalvo G, Gassner G, Mitterer C. Influence of high-temperature oxide formation on the tribological behaviour of TiN and VN coatings. *Wear* 2007;262(9–10):1152–8.
- [30] Aouadi SM, Luster B, Kohli P, Muratore C, Voevodin AA. Progress in the development of adaptive nitride-based coatings for high temperature tribological applications. *Surf Coat Technol* 2009;204(6–7):962–8.
- [31] Aouadi SM, Gao H, Martini A, Scharf TW, Muratore C. Lubricious oxide coatings for extreme temperature applications: A review. *Surf Coat Technol* 2014;257:266–77.
- [32] Xu YX, Hu C, Chen L, Pei F, Du Y. Effect of V-addition on the thermal stability and oxidation resistance of CrAlN coatings. *Ceram Int* 2018;44(6):7013–9.
- [33] Wang C, Xu B, Wang Z, Li H, Wang L, Chen R, et al. Tribological mechanism of (Cr, V) N coating in the temperature range of 500–900 °C. *Tribol Int* 2021;159:106952.
- [34] Lugscheider E, Knotek O, Bärfwulf S, Bobzin K. Characteristic curves of voltage and current, phase generation and properties of tungsten-and vanadium-oxides deposited by reactive dc-MSIP-PVD-process for self-lubricating applications. *Surf Coat Technol* 2001;142:137–42.
- [35] Mitterer C, Fateh N, Munnik F. Microstructure–property relations of reactively magnetron sputtered VCxNy films. *Surf Coat Technol* 2011;205(13–14):3805–9.

- [36] Perfiljev V, Moshkovich A, Lapsker I, Laikhtman A, Rapoport L. The effect of vanadium content and temperature on stick-slip phenomena under friction of CrV (x) N coatings. *Wear* 2013;307(1–2):44–51.
- [37] Franz R, Mitterer C. Vanadium containing self-adaptive low-friction hard coatings for high-temperature applications: A review. *Surf Coat Technol* 2013;228:1–13.
- [38] Bondarev AV, Kvashnin DG, Shchetinin IV, Shtansky DV. Temperature-dependent structural transformation and friction behavior of nanocomposite VCN-(Ag) coatings. *Mater Des* 2018;160:964–73.
- [39] Tillmann W, Hagen L, Kokalj D, Paulus M, Tolan M. Temperature-induced formation of lubricious oxides in vanadium containing iron-based arc sprayed coatings. *Coatings* 2019;9(1):18.
- [40] Ponomarev I, Polcar T, Nicolini P. Tribological properties of V2o5 studied via reactive molecular dynamics simulations. *Tribol Int* 2021;154:106750.
- [41] Fernandes F, Morgiel J, Polcar T, Cavaleiro A. Oxidation and diffusion processes during annealing of TiSi (V) N films. *Surf Coat Technol* 2015;275:120–6.
- [42] Fernandes F, Loureiro A, Polcar T, Cavaleiro A. The effect of increasing V content on the structure, mechanical properties and oxidation resistance of Ti-Si-V-N films deposited by DC reactive magnetron sputtering. *Appl Surf Sci* 2014;289:114–23.
- [43] Van Duin AC, Dasgupta S, Lorant F, Goddard WA. Reaxff: a reactive force field for hydrocarbons. *J Phys Chem A* 2001;105(41):9396–409.
- [44] Chenoweth K, Van Duin AC, Persson P, Cheng M-J, Oxgaard J, Goddard Iii WA. Development and application of a ReaxFF reactive force field for oxidative dehydrogenation on vanadium oxide catalysts. *J Phys Chem C* 2008;112(37):14645–54.
- [45] Jeon B, Ko C, Van Duin AC, Ramanathan S. Chemical stability and surface stoichiometry of vanadium oxide phases studied by reactive molecular dynamics simulations. *Surf Sci* 2012;606(3–4):516–22.
- [46] Aktulga HM, Fogarty JC, Pandit SA, Grama AY. Parallel reactive molecular dynamics: Numerical methods and algorithmic techniques. *Parallel Comput* 2012;38(4–5):245–59.
- [47] Plimpton S. Fast parallel algorithms for short-range molecular dynamics. *J Comput Phys* 1995;117(1):1–19.
- [48] Thompson AP, Aktulga HM, Berger R, Bolintineanu DS, Brown WM, Crozier PS, et al. LAMMPS—a flexible simulation tool for particle-based materials modeling at the atomic, meso, and continuum scales. *Comput Phys Comm* 2021;108171.
- [49] Lu X, Khonsari MM, Gelinck ERM. The stribeck curve: Experimental results and theoretical prediction. *J Tribol* 2006;128(4):789–94.
- [50] Seeton CJ. Viscosity-temperature correlation for liquids. In: *International joint tribology conference*, Vol. 42592, 2006. p. 131–42.
- [51] Ojovan MI. Viscosity and glass transition in amorphous oxides. *Adv Condens Matter Phys* 2008;2008.
- [52] Fateh N, Fontalvo G, Gassner G, Mitterer C. The beneficial effect of high-temperature oxidation on the tribological behaviour of V and VN coatings. *Tribol Lett* 2007;28(1):1–7.
- [53] Ogletree D, Carpick RW, Salmeron M. Calibration of frictional forces in atomic force microscopy. *Rev Sci Instrum* 1996;67(9):3298–306.
- [54] Carpick RW, Salmeron M. Scratching the surface: fundamental investigations of tribology with atomic force microscopy. *Chem Rev* 1997;97(4):1163–94.
- [55] Gao J, Luedtke W, Gourdon D, Ruths M, Israelachvili J, Landman U. Frictional forces and Amontons' law: from the molecular to the macroscopic scale. *J Phys Chem B* 2004;108(11):3410–25.
- [56] Fan C, Liaw P, Liu C. Atomistic model of amorphous materials. *Intermetallics* 2009;17(1–2):86–7.
- [57] Wang Y, Sakamaki T, Skinner LB, Jing Z, Yu T, Kono Y, et al. Atomistic insight into viscosity and density of silicate melts under pressure. *Nature Commun* 2014;5(1):1–10.
- [58] Bauchy M, Micoulaut M. Atomic scale foundation of temperature-dependent bonding constraints in network glasses and liquids. *J Non-Crystall Solids* 2011;357(14):2530–7.
- [59] Humphrey W, Dalke A, Schulten K. VMD: visual molecular dynamics. *J Mol Graph* 1996;14(1):33–8.